Crystal and magnetic structure of La$_{1-x}$Sr$_{1+x}$MnO$_4$: role of the orbital degree of freedom

D. Senff,[1] P. Reutler,[2,3] M. Braden,[1,*] O. Friedt,[1] D. Bruns,[1,2] A. Cousson,[4] F. Bourée,[4] M. Merz,[5] B. Büchner,[6] and A. Revcolevschi[3]

[1]*II. Physikalisches Institut, Universität zu Köln, Zülpicher Str. 77, D-50937 Köln, Germany*
[2]*II. Physikalisches Institut, RWTH Aachen, Huykensweg D-52056 Aachen, Germany*
[3]*Laboratoire de Physico-Chimie de l'Etat Solide, Université Paris Sud, 91405 Orsay Cedex, France*
[4]*Laboratoire Léon Brillouin, C.E.A./C.N.R.S., F-91191 Gif-sur-Yvette Cedex, France*
[5]*Institut für Kristallographie, RWTH Aachen, D-52056 Aachen, Germany*
[6]*IFW-Dresden, Helmholtzstrasse 20, D-01069 Dresden, Germany*
(Dated: February 2, 2008, **preprint**)

The crystal and magnetic structure of La$_{1-x}$Sr$_{1+x}$MnO$_4$ ($0 \leq x \leq 0.7$) has been studied by diffraction techniques and high resolution capacitance dilatometry. There is no evidence for a structural phase transition like those found in isostructural cuprates or nickelates, but there are significant structural changes induced by the variation of temperature and doping which we attribute to a rearrangement of the orbital occupation.

I. INTRODUCTION

Manganates have drawn a large interest due to the observation of a colossal magneto-resistivity in RE$_{1-x}$(Sr/Ca)$_x$MnO$_3$ and in La$_{2-2x}$Sr$_{1+2x}$Mn$_2$O$_7$.[1,2] The magnetoresistivity appears to result from the competition between the ferromagnetic metallic state and the ordering of charge, orbital and magnetic degrees of freedom. The single layer materials La$_{1-x}$Sr$_{1+x}$MnO$_4$, of the K$_2$NiF$_4$-structure type, have been much less studied, because in these compounds high magnetic fields of the order of 30 T are needed to induce a large magneto-resistivity.[3] The high value of the transition field, however, indicates that the complex ordered state is particularly stable in the single layer manganates. Many techniques have been applied to characterize the order in the half-doped layered compound La$_{0.5}$Sr$_{1.5}$MnO$_4$.[4,5,6,7,8]

The composition La$_{1.0}$Sr$_{1.0}$MnO$_4$ corresponds to LaMnO$_3$ in the perovskite series, since all Mn ions are three-valent. Like the perovskite LaMnO$_3$, La$_{1.0}$Sr$_{1.0}$MnO$_4$ exhibits an antiferromagnetic order. Kawano et al. report a small ordered moment of only 0.8 μ_B[9] compared to the value of 3.87(3) observed in LaMnO$_3$.[10] A more recent study on La$_{1.0}$Sr$_{1.0}$MnO$_4$ finds a larger moment of 3.3μ_B.[11] Through the substitution of La by divalent Sr, part of the Mn is oxidized, which may suggest physics similar to that of the perovskite materials based on the Zener double exchange mechanism. However, in the La$_{1-x}$Sr$_{1+x}$MnO$_4$ series there is no metallic ferromagnetic phase at ambient conditions. Instead, the charges, the orbital degrees of freedom and the spins order in closely coupled patterns. In this sense the La$_{1-x}$Sr$_{1+x}$MnO$_4$ phase diagram resembles that of Pr$_{1-x}$Ca$_x$MnO$_3$ where there is no metallic phase at zero magnetic field neither. Upon increasing the Sr content in La$_{1-x}$Sr$_{1+x}$MnO$_4$ the commensurate antiferromagnetic order disappears near x=0.15[12,13] and charge order appears for x larger than 0.4.[8,13] For the intermediate concentrations spin-glass behavior is observed.[13]
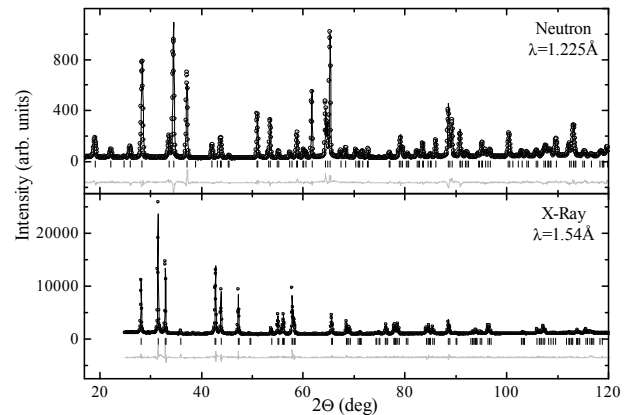

FIG. 1: Typical diffraction patterns obtained for the layered manganates : (top) a neutron powder diffraction pattern measured on the 3T.2 diffractometer for La$_{0.75}$Sr$_{1.25}$MnO$_4$; (bottom) a x-ray diffraction pattern determined on a D5000-diffractometer. Points designate the intensity data, dark lines the profile fits and fine lines the intensity differences. Vertical bars indicate the the Bragg-positions.

Concerning the crystal structure, so far only the lattice parameters were determined as a function of doping.[12] Upon introduction of Sr, the c parameter decreases, whereas the in-plane parameter a increases. We have performed a systematic study of the crystal and magnetic structure of La$_{1-x}$Sr$_{1+x}$MnO$_4$ by neutron and by x-ray diffraction techniques combined with measurements of the thermal expansion. We find strong evidence of an orbital rearrangement, both as a function of temperature and as a function of doping.

II. EXPERIMENTAL

Single crystals of La$_{1-x}$Sr$_{1+x}$MnO$_4$ were grown as described elsewhere.[14] Powder samples were obtained by

crushing single crystalline samples with a poor mosaic spread. Magnetic properties of the samples were reported by Baumann et al..[15] The crystal and magnetic structure of $La_{1-x}Sr_{1+x}MnO_4$ was studied by powder and by single crystal diffraction using neutrons and x-rays. All neutron experiments were performed on instruments of the Laboratoire Léon Brillouin installed at the Orphée reactor in Saclay. The crystal and magnetic structure of single crystals of composition $La_{1.0}Sr_{1.0}MnO_4$ and $La_{0.5}Sr_{1.5}MnO_4$ were studied on the neutron four-circle diffractometer 5C.2 at room temperature and at $\sim$20 K. Powder neutron diffraction experiments on samples of $La_{1-x}Sr_{1+x}MnO_4$ with x=0.125, 0.25, 0.4 and 0.6 were performed on the high resolution neutron diffractometer 3T.2 using a wavelength of 1.23 Å. The temperature dependence of the lattice parameters was studied by powder x-ray diffraction using Cu-K$_\alpha$ radiation and by measurements of the thermal expansion coefficients with a high resolution capacitance dilatometer on single crystalline samples. All diffraction patterns were analyzed by the Rietveld method using the Fullprof program.[16] Typical diffraction patterns, together with the profile-fitted description, are shown in Fig. 1. The temperature dependence of magnetic superstructure peaks was determined using the 4F triple-axis spectrometers.
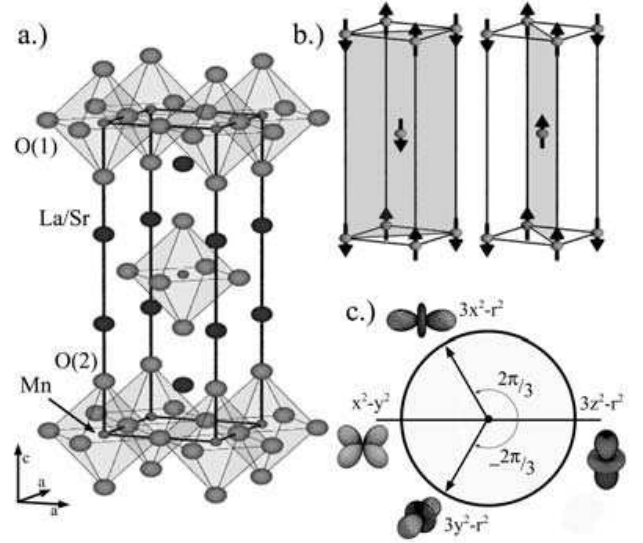

FIG. 2: a) Crystal structure of $La_{1.0}Sr_{1.0}MnO_4$ at room temperature; b) antiferromagnetic structure of $La_{1.0}Sr_{1.0}MnO_4$, the two domains are shown (the ferromagnetic planes are shaded for the two domains); c) schematic drawing of the e_g orbital state in the pseudospin space. The angles $\theta = -2\pi/3, \pi, 2\pi/3$ and 0 correspond to the $3y^2 - r^2$, $x^2 - y^2$, $3x^2 - r^2$ and $3z^2 - r^2$ orbitals, respectively.

III. MAGNETIC AND CRYSTAL STRUCTURE OF LOW-DOPED SAMPLES WITH COMMENSURATE ANTIFERROMAGNETIC ORDER

$La_{1.0}Sr_{1.0}MnO_4$ exhibits antiferromagnetic order with the magnetic moments aligned along the c axis.[9] Using a small single crystal of $\sim$10mm^3 volume a set of 1100 Bragg reflection intensities was collected on the four-circle diffractometer 5C.2 in respect with the I4/mmm lattice (dimension $3.8 \times 3.8 \times 12$Å^3). At room temperature, no evidence for superstructure reflections was found. At low temperature, superstructure intensities were found at positions ($h/2$ $k/2$ l) in respect with the I4/mmm lattice which agree with the antiferromagnetic order reported previously.[9,11,13] A set of 152 magnetic Bragg reflection intensities and 965 fundamental intensities was recorded at 20 K. Due to the high crystal quality, extinction effects turned out to be important in this experiment and that on the composition $La_{0.5}Sr_{1.5}MnO_4$, see below. Therefore, we have corrected the data for extinction using the Becker-Coppens formalism for an anisotropic mosaic spread. It is important to take into account the facts that the reliability of the determination of the strong Bragg intensities is hampered by the extinction and that the multiple diffraction may add intensity to weak reflections. Therefore, we have enhanced the statistical errors σ_{stat} by :

$$\sigma^2 = \sigma_{stat}^2 + Int. * c_{mult} + c_{const}$$

using the observed intensity Int and two additional constants c_{mult} and c_{const}, following the procedure described in detail for a similar problem.[17] In addition, reflections with an extinction correction larger than 0.75 were excluded from the refinements. Using this procedure we obtain a satisfying description of the Bragg reflections. The sets of 1037(871) reflections taken at room temperature (T=20 K) are described with reliability factors of $R_w(F^2)$=4.71%(3.16%) and $R_{unw.}(F^2)$=3.99%(3.56%). The structural results are given in Table I.

In the K_2NiF_4-structure of space group I4/mmm, there is an intrinsic difference between the antiferromagnetic ordering of spins oriented along the c direction or oriented along an in-plane direction. If the spins are oriented within the plane, the phase of the order in the neighboring plane leads to two symmetrically different phases usually called La_2CuO_4 and La_2NiO_4-type. In contrast the different phases of ordering along the c direction yield two domains of the same symmetry if the ordered moment points along the c direction. The three-dimensional coupling in $La_{1.0}Sr_{1.0}MnO_4$ arises from the coupling with the next-nearest layer, which is ferromagnetic and rather weak; the two magnetic domains are drawn in Fig. 2.

The collected magnetic Bragg intensities correspond to a superposition of contributions of both domains. The refinement of the magnetic structure was performed with the Fullprof program using the magnetic form factor of Mn^{3+} and the crystal structure determined above. The two-domain structure was taken into account. We ob-

		x=0^a	x=0.125^b	x=0.25^b	x=0.4^b	x=0.5^a	x=0.6^b
a (Å)	RT	3.786	3.814	3.846	3.857	3.863	3.857
	LT	3.768	3.794	3.840	3.852	3.855	3.857
c (Å)	RT	13.163	12.938	12.676	12.548	12.421	12.402
	LT	13.195	12.985	12.651	12.524	12.397	12.405
V (Å)^3	RT	188.676	188.204	187.500	186.670	185.356	184.498
	LT	187.348	186.879	186.588	185.855	184.257	184.555
Mn U_{iso} (10^{-4}Å^2)	RT	13(3)/68(3)^c	15(6)	18(6)	5(4)	19(2)/30(3)^c	28(5)
	LT	9(3)/30(5)^c	5(4)	29(7)	10^d	5(3)/ 5(3)^c	6(4)
La/Sr z	RT	0.35598(2)	0.35688(8)	0.35815(9)	0.35917(11)	0.35816(3)	0.35799(8)
	LT	0.35564(2)	0.35699(8)	0.35779(9)	0.35864(15)	0.35814(4)	0.35786(7)
U_{iso} (10^{-4}Å^2)	RT	46(8)/38(8)^c	34(3)	57(3)	63(3)	40(1)/30(1)^c	7(4)
	LT	19(1)/17(2)^c	18(3)	41(3)	10(4)	5(3)/ 5(3)^c	6(2)
O(1) U_{11} (10^{-4}Å^2)	RT	31(1)	46(8)	63(9)	122(9)	62(2)	67(6)
	LT	27(2)	63(8)	83(9)	43(8)	36(3)	54(6)
U_{22} (10^{-4}Å^2)	RT	71(1)	46(7)	75(8)	65(8)	69(2)	47(6)
	LT	45(2)	24(8)	87(8)	97(8)	68(3)	66(6)
U_{33} (10^{-4}Å^2)	RT	100(2)	74(8)	55(11)	94(11)	67(2)	87(7)
	LT	58(3)	62(8)	55(10)	6(10)	27(4)	42(6)
O(2) z	RT	0.17221(3)	0.16900(11)	0.16494(17)	0.16386(15)	0.16106(8)	0.15966(10)
	LT	0.17270(4)	0.17023(11)	0.16449(15)	0.16260(19)	0.16138(10)	0.15968(9)
U_{11} (10^{-4}Å^2)	RT	179(2)	191(7)	167(15)	153(7)	117(2)	93(4)
	LT	131(2)	86(6)	131(7)	134(9)	70(2)	63(4)
U_{33} (10^{-4}Å^2)	RT	74(2)	163(9)	191(11)	137(10)	68(2)	61(7)
	LT	51(3)	180(9)	185(10)	56(8)	52(3)	33(6)
Bond length $d_{\mathrm{Mn}-\varnothing(1)}$ (Å)	RT	1.89335(1)	1.90714(3)	1.92329(4)	1.92903(4)	1.93164(3)	1.92853(3)
	LT	1.88403(8)	1.89684(4)	1.92018(4)	1.92615(5)	1.92763(6)	1.92859(3)
$d_{\mathrm{Mn}-\varnothing(2)}$ (Å)	RT	2.2668(4)	2.1873(14)	2.0915(21)	2.0574(19)	2.0005(9)	1.9805(10)
	LT	2.2788(5)	2.2104(14)	2.0810(19)	2.0360(24)	2.0006(13)	1.9808(5)

^{a}Refinement of single-crystal-data ^{b}Refinement of powder-crystal-data ^{c}The single-crystal data refinement allows one to determine anisotropic thermal parameters on the Mn and La/Sr sites, U11=U22 and U33. ^{d}This value was fixed during the refinement since it tended to negative values.

TABLE I: Results of the single crystal and powder neutron diffraction experiments on La$_{1-x}$Sr$_{1+x}$MnO$_4$ for room (RT) and low temperature (LT).

tain an ordered magnetic moment of 3.21(3)μ_B in strong disagreement with a first report,[9] but in good agreement with more recent work.[11] The difference is most likely due to a poor sample quality of the crystal studied first. Our sample exhibits the antiferromagnetic ordering at T$_N$=127 K, in good agreement with the study by Moritomo et al.[13] Attempts to refine an additional ordered moment component, aligned perpendicular to the c axis, did not yield a significant value. The ordered moment is still lower than what is expected for a Mn^{3+}-ion without an orbital contribution, i.e. 4μ_B, and it is still lower than the ordered moment reported for LaMnO$_3$.[10] A part of the moment reduction may be attributed to the two-dimensional character of the antiferromagnetic coupling in La$_{1.0}$Sr$_{1.0}$MnO$_4$, but this reduction gives only $\Delta m = 0.22\mu_B$. However, there is evidence that part of the magnetic order in La$_{1.0}$Sr$_{1.0}$MnO$_4$ remains two-dimensional in character and does not transform into the 3-dimensional Bragg intensities.[18]

The crystal and magnetic structure of the La$_{0.875}$Sr$_{1.125}$MnO$_4$-sample was studied by powder neutron diffraction. We find the same magnetic super-structure peaks and obtain an ordered magnetic moment of 2.4(1)μ_B. The further reduction of the moment compared to pure La$_{1.0}$Sr$_{1.0}$MnO$_4$ agrees with the reduced Néel temperature, $T_N \sim$62 K, and the finding that, for this composition, the amount of two-dimensional diffuse magnetic scattering is further enhanced.[18]

The most interesting structural aspect concerns the elongation of the MnO$_6$ octahedron. Three-valent Mn possesses four electrons in the 3d-shell with one occupying the e_g-orbitals; therefore Mn^{3+} is strongly Jahn-Teller active, and one expects a strong octahedron elongation. In the layered material there is a competition between the crystal field of the Mn planar structure favoring an elongation along the c axis, like in La$_2$CuO$_4$ or in La$_2$NiO$_4$ (note that the octahedron in the nickelates is elongated though Ni^{2+} is not a Jahn-Teller ion),

and the exchange energy.[19] In order to allow for the virtual hopping of e_g-electrons to their nearest neighbors in the a, b-plane, it is preferable to have e_g-orbitals occupied with the lobes within this plane. Furthermore, the elastic interactions will favor an arrangement such that the long axis of one octahedron is pointing towards the short axis of an neighboring site.[20] A similar arrangement is realized in the perovskite LaMnO$_3$ in the a, b planes of the Pbnm crystal structure,[21] where it causes a ferromagnetic coupling.[10] In the layered manganate La$_{1.0}$Sr$_{1.0}$MnO$_4$, the crystal field appears to over-rule these mechanisms, since the elongation axes point along the c direction. The Mn-O bond distances at room temperature amount to 2×2.267 Å $+ 4 \times 1.893$ Å compared to 2×1.968 Å $+ 2 \times 1.907$ Å $+ 2 \times 2.178$ Å for the perovskite LaMnO$_3$.[21] The difference of the Mn-O distances is even stronger in the layered material than in LaMnO$_3$ due to the combined effect of the Jahn-Teller effect and the K$_2$NiF$_4$-structure crystal field. The ferroorbital ordering of the e_g-orbital along the c direction agrees with the antiferromagnetic ordering of the spins within the planes.

In view of the large splitting in the bond distances, one might expect a complete orbital ordering and a stable crystal structure. However, we find that the bond distances vary significantly with temperature (see Table I). The Mn-O2 to Mn-O1 distance ratio increases from 1.197(2) to 1.209(3), upon cooling from room temperature to 20 K. Further insight is obtained from the analysis of the lattice constants as a function of temperature, see Fig 3. Both, the determination of the lattice parameters by x-ray powder diffraction and the measurement of the thermal expansion coefficient with a high resolution capacitance dilatometer, yield large and anisotropic anomalies around the Néel ordering. Upon cooling, the c axis expands while the in-plane parameters shrink, in agreement with the observation of the more elongated MnO$_6$-octahedron at low temperature. The thermal expansion coefficients, corresponding to the temperature derivatives of the lattice constants, exhibit a λ-like anomaly at the Néel-temperature. In the antiferromagnetically ordered phase, the c axis expansion and the in-plane shrinking are less pronounced. The clear coupling between the structural effect and the magnetic ordering indicates an orbital origin. Most likely the orbital order is not complete in La$_{1.0}$Sr$_{1.0}$MnO$_4$, but some of the in-plane e_g-orbitals are still occupied. The anisotropic thermal expansion indicates that there is a change in the orbital occupation. Upon cooling, less in-plane orbitals are occupied. The temperature dependence of the lattice parameters suggests that the orbital rearrangement is spread over a wide temperature interval, 10–600 K. Only at very high temperatures does the c axis exhibit a normal, positive thermal expansion.

In Fig. 2 the e_g orbitals relevant in La$_{1.0}$Sr$_{1.0}$MnO$_4$ are depicted. The mixing of in-plane and out-of-plane e_g-orbitals has been modeled by a combination of the

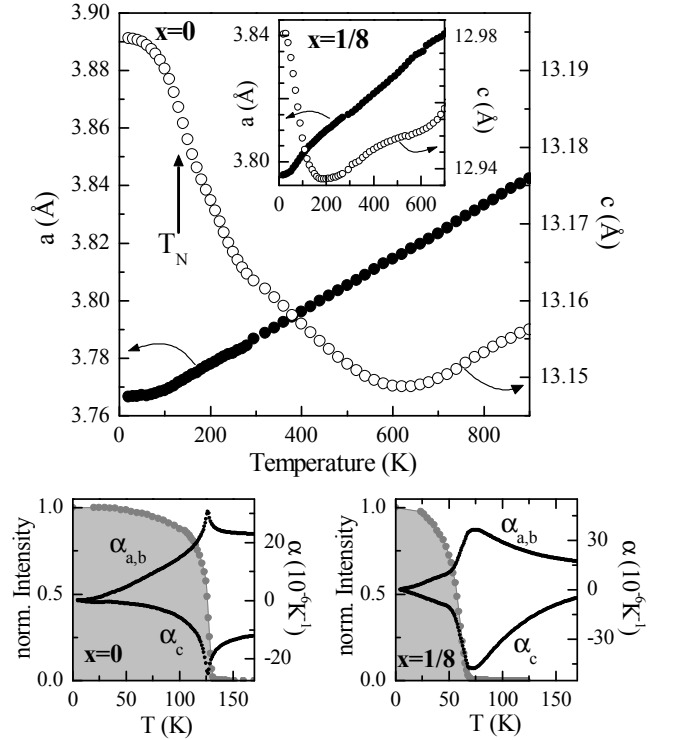FIG. 3: (Upper Panel) Temperature dependence of the lattice constants in La$_{1.0}$Sr$_{1.0}$MnO$_4$ as a function of temperature (the arrow indicates the Néel-temperature). The inset shows the temperature dependence of the lattice constants in La$_{0.875}$Sr$_{1.125}$MnO$_4$ where Néel order occurs at ~ 62 K. (Lower Panel) thermal expansion coefficient (parallel and perpendicular to the MnO$_2$ layers) determined by capacitance dilatometry and the normalized intensity of the antiferromagnetic superstructure reflection (0.5 0.5 0) measured by neutron diffraction for La$_{1.0}$Sr$_{1.0}$MnO$_4$ (left) and for La$_{0.875}$Sr$_{1.125}$MnO$_4$ (right).

$3z^2 - r^2$ and $x^2 - y^2$ orbitals,[19,22]

$$|\theta\rangle = cos(\theta/2)|3z^2 - r^2\rangle + sin(\theta/2)|x^2 - y^2\rangle.$$

The $x^2 - y^2$ and $3z^2 - r^2$ orbitals correspond to the coefficients $\theta = \pi$ and $\theta = 0$, respectively. In-plane elongated e_g-orbitals correspond to values of $\theta = \pm 2\pi/3$. With such a linear combination one assumes at least a local distortion of the tetragonal symmetry. The value of θ may fluctuate around the average value of $\theta = 0$ corresponding to the $3z^2 - r^2$-orbital. However, at the moment there is no evidence for such symmetry reduction. The orbital occupation in La$_{1.0}$Sr$_{1.0}$MnO$_4$ may eventually correspond to a linear combination with imaginary coefficients corresponding to an admixture of orbitals which would not break the local symmetry.[23]

The second sample presenting an antiferromagnetic ordering, La$_{0.875}$Sr$_{1.125}$MnO$_4$, exhibits qualitatively similar anomalies in the lattice constants. However, the anomalous c axis expansion and the in-plane shrinking occur over a smaller temperature interval upon cooling. The c parameter of La$_{0.875}$Sr$_{1.125}$MnO$_4$ increases by the same

amount between 200 and 10 K, as does the c axis in $La_{1.0}Sr_{1.0}MnO_4$ between 600 and 10 K. Concerning the effects in the in-plane parameters, it is less obvious that one may separate the electronically-induced effects from the normal thermal expansion, as they have the same sign. The thermal expansion temperature dependence, see lower part of Fig. 3, again shows the maxima just at the Néel temperature and a reduced effect in the ordered phase. So, both compositions exhibit a continuous elongation of the MnO_6 octahedron when approaching the Néel order from high temperature and this tendency gets stopped in the ordered state.

Doping $La_{1.0}Sr_{1.0}MnO_4$ with additional Sr induces Mn^{4+}-sites where no e_g-orbitals are occupied. Such Mn^{4+}-sites may attract the e_g-orbitals of neighboring Mn^{3+}-site, and the concept of an orbital polaron has been proposed.[24] In the layered material the doping-induced Mn^{4+}-sites will destabilize the ordering of the e_g-orbitals elongated along the c direction and – simultaneously – the antiferromagnetic order. The balance between the crystal field preferring a c elongation of the e_g-orbitals and the kinetic energy favoring an orientation of the orbitals along the planes, is shifted towards the in-plane orientation through the doping, since, only in this case, the e_g-electron may easily hop. Therefore, compared to $La_{1.0}Sr_{1.0}MnO_4$, there seems to be more in-plane elongated e_g-states occupied in $La_{0.875}Sr_{1.125}MnO_4$ at high temperature. The increase of the magnetic correlations induced upon cooling leads then to a redistribution of electrons which is stronger than in $La_{1.0}Sr_{1.0}MnO_4$.

The interpretation of the structural anomalies by an orbital redistribution is supported by recent x-ray absorption measurements which find a finite and temperature-dependent occupation of the e_g-orbital oriented in the planes.[25]

The anomalies in the thermal expansion suggesting a rearrangement of the orbital occupation induced by the magnetic interaction resemble recent observations on $LaTiO_3$[26,27] and on Ca_2RuO_4.[28] In these compounds, one finds an enhancement of an octahedron distortion upon approach of the Néel order. In the case of the ruthenate the accompanying change in the orbital occupation has been directly observed by x-ray absorption spectroscopy.[29] As in $La_{1.0}Sr_{1.0}MnO_4$, the octahedron distortion implies a stronger crystal field splitting of the orbital energies in these t_{2g} systems. Observing a similar effect in the strongly Jahn-Teller active e_g-system $La_{1.0}Sr_{1.0}MnO_4$ appears more astonishing.

IV. AVERAGE CRYSTAL STRUCTURE FOR INTERMEDIATE DOPING

–Crystal structure– Upon further increase of the Sr content the commensurate antiferromagnetic order, as illustrated in Fig. 2, disappears, and rather complex schemes of charge, orbital and magnetic order appear, amongst which that of the half-doped composition is
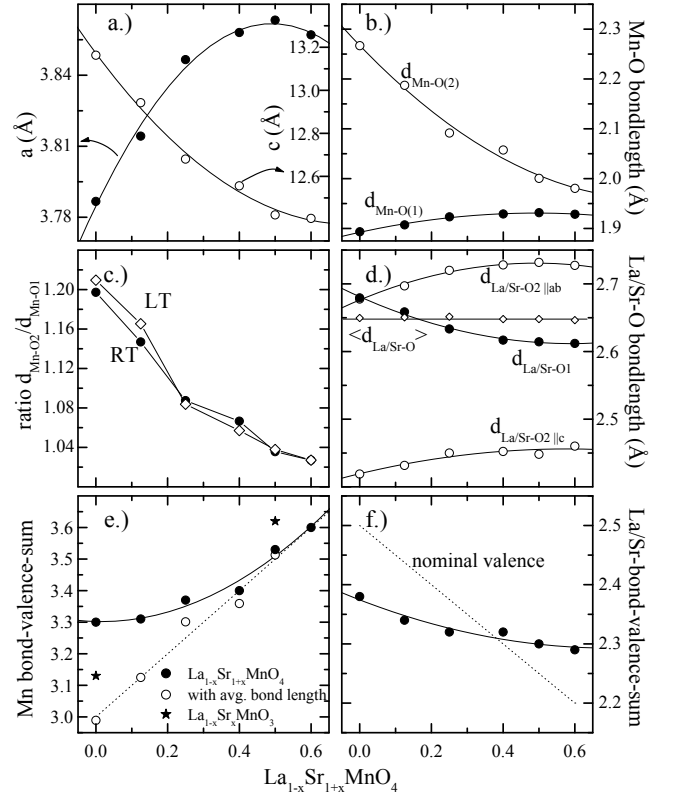

FIG. 4: Doping dependence of : the lattice parameters (a), the Mn-O bond lengths (b), the ratio of the two Mn-O bond lengths (c), the three distinct bond lengths in the (La,Sr)O_9-polyedron (d) for the series $La_{1-x}Sr_{1+x}MnO_4$. Calculated bond-valence-sum for the central Mn-ion (closed circles denote the values obtained with the split bond lengths, open circle those calculated with the average Mn-O bond length and stars values calculated for $LaMnO_3$[21] and $La_{0.5}Sr_{0.5}MnO_3$[30] e)) and for the La/Sr place (f). Drawn lines are guides to the eye.

best studied.[4,5,6,7,8] The single crystal of composition $La_{0.75}Sr_{1.25}MnO_4$ studied here does not show the superstructure peaks indexed by $(h/2\ k/2\ 1)$ but magnetic scattering at an incommensurate $\mathbf{q}$-position $(0.5, 0.16, 0)$, which one may not relate with the simple commensurate magnetic ordering.[18] With the diffraction techniques used here, we are not able to study the structural distortion arising from the charge and orbital order, we may only discuss the average crystal structure. A single crystal of $La_{0.5}Sr_{1.5}MnO_4$ was studied on the four-circle diffractometer. As extinction effects were again severe, we used the same methods as for the $La_{1.0}Sr_{1.0}MnO_4$-sample. The data sets of 1030(554) reflections taken at room temperature (T=25 K) are described with reliability factors of $R_w(F^2)=5.65\%(6.24\%)$ and $R_{unw.}(F^2)=5.65\%(6.07\%)$. The structural results are given in Table I.

The lattice constants, see Fig. 4a), show that the trend already discussed continues with a further increase of the Sr content up to $x = 0.6$. The c parameter shrinks and

the in-plane parameter slightly expands. Simultaneously, the Mn-O2 bond shrinks and the Mn-O1-bond expands (see Fig. 4b) and 4c)). The increase of the Sr content corresponds to an oxidation of the Mn-sites or to an increase in the number of Mn^{4+}-sites, which, in first view, should lead to shorter average Mn-O bond distances. The Sr dependence of the lattice constants and bond lengths indicates that this effect superposes with the one discussed above : the continuing change in the orbital occupation at the Mn^{3+}-sites. For $x = 0$ mainly the c-elongated orbitals are occupied, whereas, for $x = 0.5$, there is a strong occupation of the in-plane components. The reminiscent elongation of the MnO_6 octahedra along the c-direction at high Sr-concentrations can be understood due to the remaining influence of the planar crystal structure. Note that the non-Jahn Teller configuration $3d^8$ in La_2NiO_4 still exhibits an octahedron elongation due to the purely structural effects.[31] The temperature dependence of the bond distance ratio (see Fig. 4c)), shows that the enhancement of the octahedron elongation at low temperature occurs only in the low-doped compounds which exhibit the commensurate antiferromagnetic order.

The change of the Mn-O bond distances may be analyzed quantitatively using the bond valence sum formalism :

$$V_{Mn} = \sum_i exp\left(\frac{d_0 - d_i(Mn-O)}{B}\right),$$

where $d_0 = (1-x) \cdot 1.76\text{Å} + x \cdot 1.753\text{Å}$ and $B = 0.37\text{Å}$ are empirical parameters[32] and $d_i(Mn-O)$ denotes the six Mn-O bond distances. The Mn bond valence sums are shown in Fig. 4e); only for Sr content higher than $x = 0.4$ one does find the nominal valence, suggesting that for low doping the crystal structure exhibits an internal stress similar to the isostructural cuprates.[33] The internal stress seems to be released with further doping as the calculated bond valence sum approaches the nominal value. In Fig. 4e) we also show the bond-valence sums caluclated with the averaged Mn-O distances, which follow the nominal values. It seems that part of the internal stress is related to the strong splitting of the Mn-O bond distances, which is probably unsufficiently decribed with the bond valence scenario. For comparison we also show the bond valence sums obtained for the perovskites $La_{1-x}Sr_xMnO_3$ which are quite close to the nominal values for x=0 and 0.5.[21,30]

The La-O coordination polyhedron, too, changes significantly with Sr content, in particular the shortest La-O2 bond, parallel to the c axis, which increases rapidly with doping in the range $0 \leq x < 0.4$, see Fig. 4d). The analysis of the bond valence sums calculated via :

$$V_{La/Sr} = (0.5 - 0.5x) \times \sum_i exp\left(\frac{d_{0-La} - d_i(La/Sr-O)}{B}\right)$$
$$+ (0.5 + 0.5x) \times \sum_i exp\left(\frac{d_{0-Sr} - d_i(La/Sr-O)}{B}\right),$$

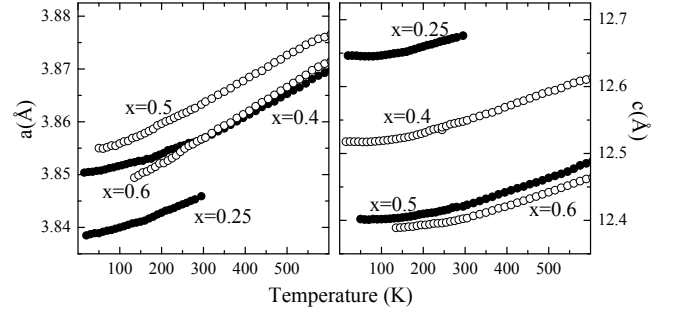is shown in Fig. 4f). At low doping, the obtained values are significantly lower than the expected values, confirm-

FIG. 5: Temperature dependence of the lattice parameters in $La_{1-x}Sr_{1+x}MnO_4$ for concentrations $x > 0.25$.

ing the interpretation that there is an internal strain in this material. This strain is reduced with doping and even turns into the opposite as the bond valence sums are larger than the expected values in the samples with Sr concentration of 0.4 or higher.

–Temperature dependence of the lattice parameters–
The temperature dependencies of the lattice constants for large doping are shown in Fig. 5. In contrast to the anomalous behavior found for the low-doped samples, the thermal expansion is quite normal in this Sr-concentration range. The complex charge, orbital and magnetic ordering schemes occurring in these samples does not imply structural changes similar to those induced through the commensurate antiferromagnetic order.

–Debye Waller factors – Our interpretation of the doping-induced reorientation of the e_g-orbitals is well supported by the anisotropic atomic displacement parameters (ADP). Due to the intrinsic disorder induced by the occupation of the same site by La and Sr, some of the displacement parameters are significantly higher than one would expect from the phonon contributions. The disorder effect has been studied in detail for $La_{2-x}Sr_xCuO_4$, where, however, only 8% of the La are replaced by Sr.[34] In $La_{1-x}Sr_{1+x}MnO_4$ the doping disorder is maximal for $La_{1.0}Sr_{1.0}MnO_4$ and decreases with further doping. Since the (La/Sr)-O bonds are perpendicular to the Mn-O bonds, the doping disorder will displace the O-atoms mainly perpendicular to the Mn-O bonds. The U_{11} parameter of O2 and the U_{33} parameter of O1 are most sensitive. These displacement parameters are indeed maximal for $x = 0$ and decrease with increasing Sr-content. The inter-atomic interaction potentials should be similar to those in $La_{2-x}Sr_xCuO_4$, therefore one may compare to the additional ADP obtained for the cuprate-system.[34] Extrapolating the disorder induced ADP contributions calculated for $La_{2-x}Sr_xCuO_4$ to x=1.0 one obtains $\Delta U_{11}(O2)=0.023\text{Å}^2$ and $\Delta U_{33}(O1)=0.0047\text{Å}^2$ and these values are of the order of the low temperature ADP's measured in $La_{1.0}Sr_{1.0}MnO_4$. The manganate seems to be less sensitive to the disorder most likely due to the more stable character of its crystal structure. In
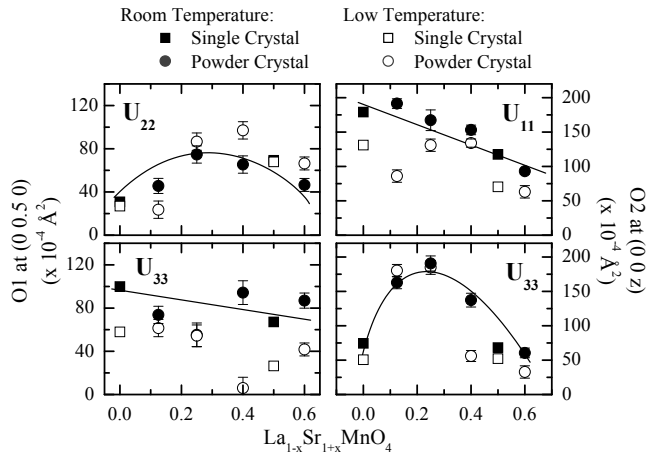
FIG. 6: Anisotropic displacement parameters of the two oxygen sites as function of temperature and doping. Note that $U_{22}(O1)$ and $U_{33}(O2)$ correspond to the displacement of the oxygen parallel to the bonds.

the $La_{1-x}Sr_{1+x}MnO_4$ phase diagram there are no structural phase transitions, whereas $La_{2-x}Sr_xCuO_4$ exhibits the octahedron tilt instabilities.

The orbital occupation is related to the atomic displacement parameters parallel to the bonds, U_{33} of O2 and the U_{22} parameter of O1. These parameters are smaller in pure $La_{1.0}Sr_{1.0}MnO_4$ than in intermediate Sr-concentrations, although the doping disorder is maximal for that composition. U_{33} of O2 exhibits a maximum around $x = 0.25$ where the orbital orientation is the less defined. This concentration roughly represents the border between the majority occupation of c-axis elongated orbitals around $La_{1.0}Sr_{1.0}MnO_4$ and the majority occu-

pation of in-plane elongated orbitals at higher doping.

The longitudinal displacement parameter of the in-plane oxygen is maximal near half-doping.[35] This finding agrees well with the model of the CE-type ordering of both the Mn^{3+}/Mn^{4+}-sites and orientation of the e_g-orbitals.[4,5,8] Both displacements have not been taken into account in our refinement of the average structure. The doping dependence of the U_{22}-O1 parameter suggests local displacements of the order of 0.1Å near half doping.

V. CONCLUSIONS

The crystal and magnetic structure of $La_{1-x}Sr_{1+x}MnO_4$ was studied by several diffraction techniques and high resolution capacitance dilatometry. At low doping $0.0 \leq x \leq 0.25$, the MnO_6 octahedra are elongated along the c direction in accordance with a majority occupation of the $3z^2 - r^2$ orbital. However, pronounced and anisotropic anomalies in the thermal expansion yield evidence that the orbital occupation varies with temperature. Upon cooling there seems to occur a shift of electrons towards the $3z^2 - r^2$ orbitals. Upon increase of the Sr-concentration, the amount of Mn^{3+} ions is reduced and the octahedron elongation along the c-direction diminishes. This effect has to be attributed to a majority occupation of the in-plane elongated e_g-orbitals, as it was predicted to arise from the magnetic coupling between Mn^{3+} and Mn^{4+} sites.[24]

* Electronic address: braden@ph2.uni-koeln.de

[1] R. von Helmolt, J. Wecker, B. Holzapfel, L. Schultz and K. Samwer, Phys. Rev. Lett. **71**, 2331 (1993); S. Jin, M. McCormack, T. H. Tiefel and R. Ramesh, J. Appl. Phys. **76**, 6929 (1994); Y. Tokura, A. Urushibara, Y. Morimoto, T. Arima, A. Asamitsu, G. Kido and N. Furukawa, J. Phys. Soc. Jpn. **63**, 3931 (1994).

[2] Y. Moritomo, A. Asamitsu, H. Kuwahara and Y. Tokura, Nature (London) **380**, 141 (1996).

[3] M. Tokunaga, N. Miura, Y. Moritomo and Y. Tokura, Phys. Rev. B **59**, 11151 (1999).

[4] B. J. Sternlieb, J. P. Hill, U. C. Wildgruber, G. M. Luke, B. Nachumi, Y. Moritomo and Y. Tokura, Phys. Rev. Lett. **76**, 2169 (1996).

[5] Y. Murakami, H. Kawada, H. Kawata, M. Tanaka, T. Arima, Y. Moritomo and Y. Tokura, Phys. Rev. Lett. **80**, 1932 (1998).

[6] B. Wilkins, P. D. Spencer, P. D. Hatton, S. P. Collins, M. D. Roper, D. Prabhakaran and A. T. Boothroyd, Phys. Rev. Lett. **91**, 167205 (2003).

[7] S. S. Dhesi, A. Mirone, C. De Nadaï, P. Ohresser, P. Bencok, N. B. Brookes, P. Reutler and A. Revcolevschi, Phys.

Rev. Lett. **92**, 056403 (2004).

[8] S. Larochelle, A. Mehta, N. Kaneko, P. K. Mang, A. F. Panchula, L. Zhou, J. Arthur and M. Greven, Phys. Rev. Lett. **87**, 095502 (2001).

[9] S. Kawano, N. Achiwa, N.Kamegashira and M. Aoki, J. de Physique **49**(C8), 829 (1988).

[10] F. Moussa, M. Hennion, J. Rodríguez-Carvajal, H. Moudden, L. Pinsard and A. Revcolevschi, Phys. Rev. B **54**, 15149 (1996).

[11] M. Bieringer and J. E. Greedan, J. Mater Chem. **12**, 279 (2002).

[12] W. Bao, C. Chen, S. Carter and S.-W. Cheong, Sol. State Commun. **98**, 55 (1995).

[13] Y. Moritomo, Y. Tomioka, A. Asamitsu, Y. Tokura and Y. Matsiui, Phys. Rev. B **51**, 3297 (1995).

[14] P. Reutler, O. Friedt, B. Büchner, M. Braden and A. Revcolevschi, Journal of Crystal Growth **249**, 222 (2003).

[15] C. Baumann, G. Allodi, B. Büchner, R. De Renzi, P. Reutler and A. Revcolevschi, Physica B **326**, 505 (2003).

[16] J. Rodríguez-Carvajal, Physica B **192**, 55(1993).

[17] M. Braden, G. Wilkendorf, J. Lorenzana, M. Ain, G.J. McIntyre, M. Behruzi, G. Heger, G. Dhalenne and A.

Revcolevschi, Phys. Rev. B **54**, 1105 (1996).

[18] D. Senff, Diploma-thesis, unpublished.

[19] D. I. Khomskii and G. Sawatzky, Sol. State Commun. **102**, 87 (1997); K. I. Kugel and D. I. Khomskii, Sov. Phys. Usp. **25**, 231 (1982).

[20] D.I. Khomskii and K. I. Kugel, Phys. Rev. B **67**, 134401 (2003).

[21] J. Rodríguez-Carvajal, F. Moussa, M. Hennion, H. Moudden, L. Pinsard and A. Revcolevschi, Phys. Rev. B **57**, 3189 (1998)

[22] T. Nagai, T. Kimura, A. Yamazaki, Y. Tomioka, K. Kimoto, Y. Tokura and Y. Matsui, Phys. Rev. B **68**, 092405 (2003).

[23] J. van den Brink and D. Khomskii, Phys. Rev. B **63**, 140416(R) (2001)

[24] G. Khilian and G. Khaliullin, Phys. Rev. B **60**, 13458 (1999); T. Mizokawa, D. I. Khomskii and G. Sawatzky, Phys. Rev. B **63**, 24403 (2000).

[25] M. Merz, unpublished results.

[26] J. Hemberger, H.-A. Krug von Nidda, V. Fritsch, J. Deisenhofer, S. Lobina, T. Rudolf, P. Lunkenheimer, F. Lichtenberg, A. Loidl, D. Bruns, and B. Büchner, Phys. Rev. Lett. **91**, 066403 (2003).

[27] M. Cwik, T. Lorenz, J. Baier, R. Müller, G. André, F. Bourée, F. Lichtenberg, A. Freimuth, R. Schmitz, E. Müller-Hartmann and M. Braden, Phys. Rev. B **68**,

[28] 060401(R) (2003).

[28] M. Braden, G. André, S. Nakatsuji and Y. Maeno, Phys. Rev. B **58**, 847 (1998); O. Friedt, M. Braden, G. André, P. Adelmann, S. Nakatsuji and Y. Maeno, Phys. Rev. B **63**, 174432(2001).

[29] T. Mizokawa, L. H. Tjeng, G. A. Sawatzky, G. Ghiringhelli, O. Tjernberg, N. B. Brookes, H. Fukazawa, S. Nakatsuji and Y. Maeno Phys. Rev. Lett. **87**, 077202 (2001).

[30] P. G. Radaelli, D. E. Cox, M. Marezio and S-W. Cheong, Phys. Rev. B **55**, 3015(1997).

[31] J. D. Jorgensen, B. Dabrowski, S. Pei, D. R. Richards and D. G. Hinks Phys. Rev. B **40**, 2187 (1989).

[32] I.D. Brown and D. Altermatt, Acta Crystal. B **41**, 244 (1985).

[33] M. Braden, P. Schweiss, G. Heger, W. Reichardt, Z. Fisk, K. Gamayunov, I. Tanaka and H. Kojima, Physica C **223**, 396 (1994).

[34] M. Braden, M. Meven, W. Reichardt, L. Pintschovius, M. T. Fernandez-Diaz, G. Heger, F. Nakamura and T. Fujita, Phys. Rev. B **63**, 140510 (2001).

[35] This conclusion is in particular supported by the neutron single crystal data, which yield more reliable ADPs. Additional studies by x-ray single crystal diffraction[25] confirm the ADP's qualitatively.